

COMBINED REFLECTANCE AND EMITTANCE SPECTROSCOPY IN THE THERMAL INFRARED BAND: IMPLICATIONS FOR MERCURY. K. S. Wohlfarth¹, A. Grumpe¹, C. Wöhler¹, A. Morlok², H. Hiesinger² ¹Image Analysis Group, TU Dortmund University, 44227 Dortmund, Germany {[kay.wohlfarth](mailto:kay.wohlfarth@tu-dortmund.de), [arne.grumpe](mailto:arne.grumpe@tu-dortmund.de), [christian.woehler](mailto:christian.woehler@tu-dortmund.de)}@tu-dortmund.de ²Institut für Planetologie, WWU, 48149 Münster, Germany

Introduction: Spectral unmixing, i.e. the recovery of the surface's composition from spectral measurements, has been applied to the near infrared domain by many researchers [e.g. 1,2,3]. Spectral measurements in the thermal infrared region (TIR) (2 μm – 20 μm) are subject to the superposition of solar reflection and variable thermal emission [4]. TIR spectra have been used to quantify modal abundances on Mars from Thermal Emission Imaging System (TEMIS) and Thermal Emission Spectrometer (TES) data [5,6]. The BepiColombo spacecraft will carry the TIR spectrometer MERTIS [7]. The contribution of this work is three-fold: Firstly, we propose a framework derived from Hapke's approach [8] to model the combined reflectance and emittance behavior of particulate media at different temperatures. Secondly, selected radiance spectra of silicates are simulated for different temperature environments in TIR, comparable to those which are expected on the Mercurian surface. Thirdly, an analysis is carried out to quantify the contributions of reflectance and emittance at different temperatures. This will lay the foundations for further research on radiance spectroscopy and spectral unmixing of silicates in the TIR region, relevant for studies of the Mercurian surface.

Method:

Model. Two types of radiation contribute to the wavelength-dependent radiance I which arrives at the sensor, i.e. reflection and emission. Collimated irradiance J hits the surface and is reflected according to a reflectance function $r(i, e, g)$. This process depends on the incidence angle i , the emission angle e and the phase angle g . Simultaneously, the body emits thermal radiation U according to Planck's law, mitigated by the directional emissivity ϵ_d :

$$I(i, e, g, \lambda) = Jr(i, e, g, \lambda) + \epsilon_d(e, \lambda)U(T, \lambda)$$

For the reflectance function r we make use of the anisotropic reflectance model proposed in [9]. The relationship between directional emissivity and directional hemispherical reflectance r_{dh} is given by

$$\epsilon_d(i, e, g, \lambda) = 1 - r_{\text{dh}}(i, e, g, \lambda)$$

For obtaining r_{dh} , we integrate the incidence angle of the reflectance function over the half sphere, extending the approach of [9]. This yields a full model for

combined reflectance and emission under arbitrary illumination conditions and temperatures.

Simulation. We start from the laboratory reflectance measurements of silicates described in [3] and apply our model to retrieve the single scattering albedo w of the specific material by nonlinear optimization. In total, we studied seven pure minerals and 21 different mixtures (Table 1) with $i=15^\circ$ and $e=15^\circ$.

Table 1. Measurement of different minerals

Mineral	Mixtures
Augite (Au)	20% Au + 30% Pa + 50% La
Diallagite (Di)	
Pargasite (Pa)	{10,20,30,70,80,90}% Pa + {90,80,70,30,20,10}% La
Ferrosilite (Fs)	50% Fs + 50% {Au,Di,Pa,La,Ol}
Ilmenite (Il)	{20,40,50,60}% Il + {80,60,50,40}% Pa, 50% Il+50% {Pa,Fs,La,Ol}
Labradorite (La)	50% La + 50% Pa
Olivine (Ol)	

The sample-specific w spectrum is subsequently fed into the whole model alongside the temperature, the illumination conditions and the material-specific phase function, which we adopt from [3] and set constant for all materials. This results in combined reflectance and emittance spectra for the initial probe under any user-defined illumination conditions and temperatures. In order to compare mixtures of reflectance and emittance spectra more easily, the radiance is then normalized and termed relative radiance I_{rel} with

$$I_{\text{rel}} = \frac{J_m r(i, e, g) + \epsilon_d(e)U(T)}{J_m + U(T)}$$

In the case only reflected light or thermal emission occurs, the expression yields normalized pure reflectance spectra or normalized pure emission spectra, respectively. Anything in between will have variable contributions of both. The solar irradiance of the Mercurian surface is calculated via the blackbody radiation of the sun, adjusted by the ratio of the squared solar radius and the squared average distance from sun to Mercury.

$$J_m = J_s \frac{R_s^2}{R_m^2}$$

Due to its vicinity to the sun, the maximum temperature of Mercury rises up to 700 K at (0°W 0°N) [10]. A mercurian day lasts nearly 88 Earth days. In this comparatively long period, the dark side of the planet is not exposed to direct solar light and the surface temperature will drop to 80 K [10]. The diurnal average temperature is 340 K [10]. To cover the whole range, simulations are carried out for the range 80 - 700 K. The model of [11] and [12] give the spatially variant temperature of Mercury’s surface, which will be of use when analyzing spectra at a given location.

Results: The simulations are exemplified based on the measured spectrum of labradorite for $i=15^\circ$ and $e=15^\circ$.

Maximum temperature. Fig. 1 depicts the thermal emission $U(T)$ at 700 K (blue, dash dotted) and solar radiation J (red, dashed) at the mercurian surface in the TIR region. For wavelengths exceeding $5 \mu\text{m}$, the $U(T)$ is more than two orders of magnitude stronger than J . Fig. 2 shows a measured reflectance spectrum (r_d) of labradorite in red (dashed) and the simulated and normalized emissivity spectrum (ϵ_d) in blue (dash dotted). The orange curve is the simulated relative radiance at 700 K which approaches the emissivity, particularly at wavelengths longer than $5 \mu\text{m}$. This clearly suggests that it is possible to treat the radiance as pure emission for a wavelength larger than $5 \mu\text{m}$.

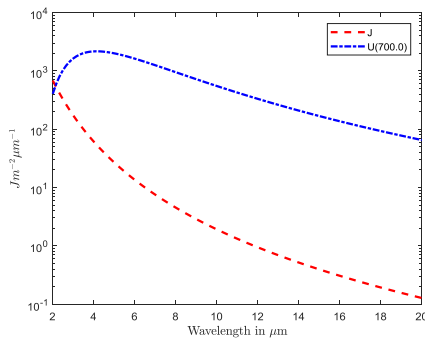


Figure 1. Approximate radiance of Mercury’s surface due to expected solar irradiation (blue) and thermal emission spectrum (green) at 700 K in the TIR range

Full Temperature Range. Figure 3 shows the simulated relative radiance spectra in the range 80 – 700 K. We observe a temperature variant change of the spectral shape which lies between the extremes of pure emissivity or pure reflectance spectra. It can be seen that decreasing temperatures result in increasing contribution of reflectance and decreasing contribution of emissivity. At very low temperatures (80 K), the spectrum behaves almost like a pure reflectance spectrum for wavelengths below $14 \mu\text{m}$. Due to the fact that the temperatures in the simulation are essentially the same

as on Mercury, a similar spectral behavior is expected on its surface.

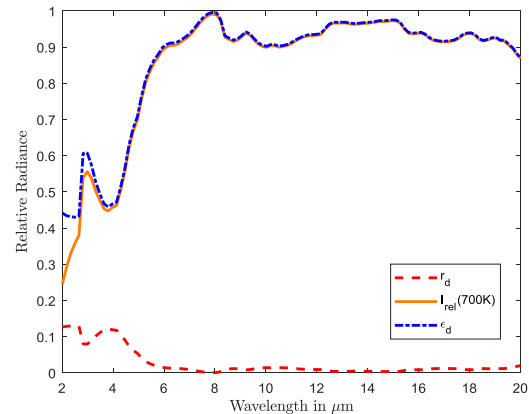


Figure 2. Measured reflectance spectrum of labradorite (red), simulated emissivity spectrum (blue) and relative radiance (orange) at 700 K

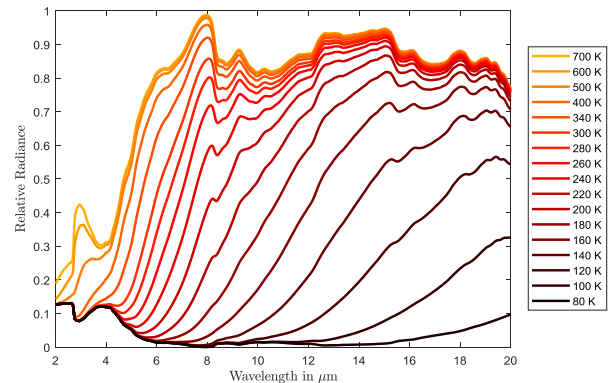


Figure 3. Simulated relative radiance spectra of labradorite in the range 80 – 700 K

Application to spectral unmixing: Spectral unmixing procedures such as [3] rely on the single scattering albedo w . To retrieve this quantity, it is crucial to precisely know the radiance coming from the planetary body. Since there are significant temperature dependent changes in TIR for mercurian surface radiance, it is necessary to apply the full described framework prior to applying spectral unmixing techniques.

References:

[1] Hiroi and Pieters (1994) *JGR: Planets*, 99, 10,867–10,879 [2] Keshava (2003) *IEEE Signal Processing Magazine*, 19, 44–57. [3] Rommel, D. et al. (2017) *Icarus*, 284, 126–149. [4] Collins, E. F. et al. (1999) *SPICE* 3753, 286–299. [5] Huang, J. et al. (2013) *JGR: Planets*, 118, 2146–2152. [6] Goudge, T. A. et al. (2015) *Icarus*, 250, 165–187. [7] Helbert, J. et al. (2005) *LPSC XXXVI*, abstract #1753 [8] Hapke, B. (2012) Cambridge University Press. [9] Hapke, B. (2002) *Icarus*, 157, 523–534. [10] Vasavada A. R. et al. (1999) *Icarus*, 141, 179–193. [11] Emery J. P. et al. (1998) *Icarus*, 136, 104–123. [12] Bauch K. et al. (2014) *Planetary and Space Science*, 101, 27-36